Convergence and Error Bound Analysis for the Space-Time CESE Method

Daoqi Yang,[1] **Shengtao Yu,**[2] **Jennifer Zhao**[3]

[1] *Department of Mathematics*
Wayne State University
Detroit, MI 48202

[2] *Department of Mechanics*
Wayne State University
Detroit, MI 48202

[3] *Department of Mathematics and Statistics*
University of Michigan–Dearborn
Dearborn, MI 48128

Received 17 September 1999; accepted 31 August 2000

In this work, we study the convergence behavior of a recently developed space-time conservation element and solution element method for solving conservation laws. In particular, we apply the method to a one-dimensional time-dependent convection-diffusion equation possibly with high Peclet number. We prove that the scheme converges and we obtain an error bound. This method performs well even for strong convection dominance over diffusion with good long-time accuracy. Numerical simulations are performed to verify the results. © 2001 John Wiley & Sons, Inc. Numer Methods Partial Differential Eq 17: 64–78, 2001

Keywords: Space-time CESE method; $\alpha - \mu$ scheme; convection diffusion equation

I. INTRODUCTION

In this article, we study the convergent behavior of a recently developed numerical method: the space-time conservation element and solution element method (the space-time CESE). This new method is proposed in [1] for conservation laws and has substantial differences in both concept and methodology from well-known methods for solving conservation laws, such as finite difference, finite volume, and finite element methods.

Mathematically, conservation laws are represented by a set of integral equations. The differential form of these laws is obtained from the integral form with the assumption that the physical

Correspondence to: Jennifer Zhao, Dept. of Mathematics and Statistics, Univ. of Michigan-Dearborn, 4901 Evergreen Rd, Dearborn, MI 48128 (e-mail: xich@umich.edu, http://www.umd.umich.edu/~xich)

solution is smooth. But, for a physical solution in a region of rapid change, this smoothness assumption may be difficult to realize. Thus, a method designed to obtain numerical solutions to the differential form without enforcing flux conservation may be at a fundamental disadvantage in modeling many physical phenomena, especially when obtaining accurate solutions for local and long-time behaviors. By contrast, the space-time CESE method was developed to enforce flux-conservation locally and globally in space and time. It always retains the basic physical reality of flux conservation, even in a region involving discontinuities. In summary, the space-time CESE method has the following major advantages. First, it enforces both local and global flux conservation in space and time. Second, space and time are unified and are treated on the same footing. Third, dependent variables and their derivatives are solved simultaneously with comparable accuracy.

The goal of this article is to conduct convergence and error bound analysis for this method. To our best knowledge, this work is the first approach in this direction. In order to provide a clear description of the method and conduct our study without involving too many technical difficulties, we carry out our study by applying the space-time CESE method to the following one-dimensional time-dependent convection-diffusion equation with possible convection dominance over diffusion:

$$\frac{\partial u}{\partial t} + a\frac{\partial u}{\partial x} - \mu\frac{\partial^2 u}{\partial x^2} = 0. \tag{1.1}$$

As shown in the next section, the $a - \mu$ scheme thus obtained is explicit and has two independent marching variables. It has the unusual property that its stability condition is independent of the diffusion coefficient μ, and there are no more mesh requirements other than the stability condition for convergence. We prove that this scheme is convergent, and that the global error for the solution in L^2 norm of space is of order Δx.

Most related works can be found in [1] and [2]. In [1], the $a - \mu$ scheme is derived and its stability is discussed. In both [1] and [2], the space-time CESE method is extended to other equations, such as the 1D time-dependent Navier–Stokes equations of a perfect gas, and the 1D convection-diffusion equation of nonconstant velocity and viscosity coefficients. There is not much mathematical study to the method in [1] or [2]; that is what this article is for. The order of the article is organized as following. In Section II, we describe the $a - \mu$ scheme. In Section III, we prove its convergence and derive an error bound. Numerical simulations are performed in Section IV.

II. $A - \mu$ SCHEME

In this section, we apply the space-time CESE method proposed in [1] to the following Cauchy problem of one-dimensional convection-diffusion equation:

$$\frac{\partial u}{\partial t} + a\frac{\partial u}{\partial x} - \mu\frac{\partial^2 u}{\partial x^2} = 0, 0 < t < T, u(x,0) = u_0(x), \tag{2.1}$$

where a is the convection velocity, $\mu > 0$ is the diffusion coefficient, both are assumed to be constants, and T is a positive constant representing the simulation ending time.

Let $x_1 = x, x_2 = t$ be considered as the coordinates in the half-plane of a two-dimensional Euclidean space $R^2_+ = \{(x,t) : -\infty < x < \infty, 0 \le t < \infty\}$. Using the Gauss divergence theorem in R^2_+, Eq. (2.1) can be written as the differential form of the following conservation

law:

$$\int_{S(V)} \vec{h} \cdot \vec{ds} = 0. \tag{2.2}$$

Here $S(V)$ is the boundary of an arbitrary space-time region V in $R^2_+, \vec{h} = (au - \mu \frac{\partial u}{\partial x}, u)$ is a current density vector in $R^2_+, \vec{ds} = d\sigma \vec{n}$ with $d\sigma$ and $\vec{n}$ being, respectively, the area and the outward unit normal of a surface element on $S(V)$.

We use Δx to represent the space grid size, Δt the time grid size, and (x_j, t^n) a particular grid point, where

$$x_j = j\Delta x, -\infty < j < +\infty, t^n = n\Delta t, n \geq 0, \tag{2.3}$$

see Fig. 1. We denote by $SE(j, n)$ the interior of a space-time region bounded by a dashed curve and call it a solution element at grid point (x_j, t^n); see Fig. 2(A). For our discussion, the exact size of this region does not matter. For any $(x, t) \in SE(j, n)$, we use $U(x, t; j, n)$ and $\vec{H}(x, t; j, n)$ to approximate $u(x, t)$ and $\vec{h}(x, t)$:

$$U(x, t; j, n) = U^n_j + (U_x)^n_j (x - x_j) + (U_t)^n_j (t - t^n), (x, t) \in SE(j, n), \tag{2.4}$$

where U^n_j, $(U_x)^n_j$, and $(U_t)^n_j$ are independent constants in $SE(j, n)$, which approximate $u(x_j, t^n)$, $u_x(x_j, t^n)$, and $u_t(x_j, t^n)$, respectively. We require $U(x, t; j, n)$ to satisfy (2.1) within $SE(j, n)$, this implies that

$$(U_t)^n_j = -a(U_x)^n_j. \tag{2.5}$$

Therefore,

$$U(x, t; j, n) = U^n_j + (U_x)^n_j ((x - x_j) - a(t - t^n)), (x, t) \in SE(j, n). \tag{2.6}$$

We also define

$$\vec{H}(x, t; j, n) = (aU(x, t; j, n) - \mu U_x(x, t; j, n), U(x, t; j, n)). \tag{2.7}$$

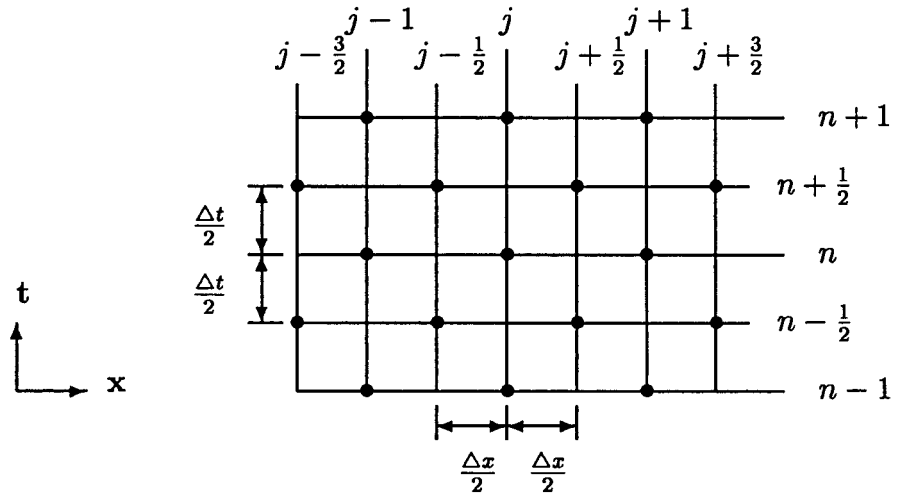

FIG. 1. Staggered grids at full and half steps.

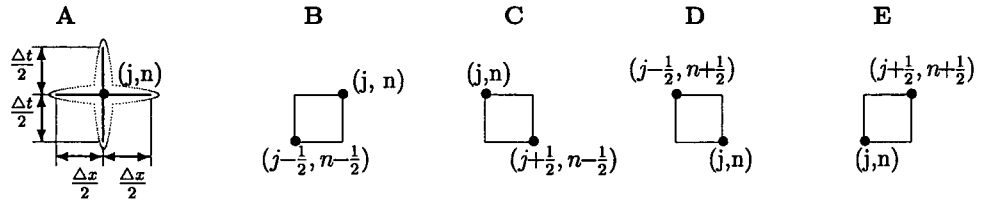

FIG. 2. Solution elements and conservation elements.

Let R_+^2 be divided into nonoverlapping rectangular regions referred to as conservation elements (CE). The CE with its top-right vertex being the mesh point $(j,n) \in \Omega$ is denoted by $CE_-(j,n)$; see Fig. 2(B), and the CE whose top-left vertex is the mesh point (j,n) is denoted by $CE_+(j,n)$; see Fig. 2(C). Similarly $CE_+(j-1/2, n+1/2)$ is illustrated in Fig. 2(D) and $CE_-(j+1/2, n+1/2)$ is illustrated in Fig. 2(E). We approximate (2.2) by

$$F_+(j,n) = \int_{S(CE_+(j,n))} \vec{H} \cdot \vec{ds} = 0, F_-(j,n) = \int_{S(CE_-(j,n))} \vec{H} \cdot \vec{ds} = 0. \tag{2.8}$$

Because each $S(CE_\pm(j,n))$ is a simple closed curve in R_+^2, the surface integral in (2.8) can be converted to a line integral. Let

$$\vec{G} = (-U, aU - \mu U_x), \vec{dr} = (dx, dt). \tag{2.9}$$

Then

$$\vec{H} \cdot \vec{ds} = \pm \vec{G} \cdot \vec{dr}. \tag{2.10}$$

Therefore,

$$F_+(j,n) = \int_{S(CE_+(j,n))} \vec{G} \cdot \vec{dr}, F_-(j,n) = \int_{S(CE_-(j,n))} \vec{G} \cdot \vec{dr}, \tag{2.11}$$

with the understanding that the integral is evaluated in the counterclockwise direction. By evaluating (2.11), we have that

$$\frac{4}{(\Delta x)^2} F_\pm(j,n) = \pm \frac{1}{2}[(1 - \tau^2 + \delta)(U_x)_j^n + (1 - \tau^2 - \delta)(U_x)_{j\pm 1/2}^{n-1/2}] + \frac{2(1 \pm \tau)}{\Delta x} (U_j^n - U_{j\pm 1/2}^{n-1/2}), \tag{2.12}$$

where

$$\tau = \frac{a\Delta t}{\Delta x}, \delta = \frac{4\mu \Delta t}{\Delta x^2}. \tag{2.13}$$

If we define

$$\vec{q}(j,n) = \begin{pmatrix} U_j^n \\ \frac{\Delta x}{4} (U_x)_j^n \end{pmatrix}, \tag{2.14}$$

then solving the two equations:

$$\frac{4}{(\Delta x)^2} F_+(j,n) = 0, \frac{4}{(\Delta x)^2} F_-(j,n) = 0, \tag{2.15}$$

leads to the $a-\mu$ scheme:

$$\vec{q}(j,n)=Q_+^2\vec{q}(j-1,n-1)+(Q_+Q_-+Q_-Q_+)\vec{q}(j,n-1)+Q_-^2\vec{q}(j+1,n-1), \quad (2.16)$$

where

$$Q_+=\frac{1}{2}\begin{pmatrix} 1+\tau & 1-\tau^2-\delta \\ \frac{-(1-\tau^2)}{1-\tau^2+\delta} & -\frac{(1-\tau)(1-\tau^2-\delta)}{1-\tau^2+\delta}\end{pmatrix}, Q_-=\frac{1}{2}\begin{pmatrix} 1-\tau & -(1-\tau^2-\delta) \\ \frac{1-\tau^2}{1-\tau^2+\delta} & -\frac{(1+\tau)(1-\tau^2-\delta)}{1-\tau^2+\delta}\end{pmatrix}. \quad (2.17)$$

This scheme is explicit and has two independent marching variables U_j^n and $\frac{\Delta x}{4}(U_x)_j^n$. We take the following initial data for (2.16):

$$U_j^0=u_0(x_j),(U_x)_j^0=\frac{\partial u_0(x_j)}{\partial x}. \quad (2.18)$$

III. CONVERGENCE AND ERROR BOUND ANALYSIS

In this section, we show that the $a-\mu$ scheme (2.16) converges and we derive its exact rate of convergence (error bound). We first give the following stability result.

Lemma 3.1. *The $a-\mu$ scheme* (2.16) *is stable if and only if*

$$1-\tau^2+\delta\neq 0,\tau^2<1. \quad (3.1)$$

Proof. The proof follows from a standard Von Neumann analysis. For details, please see [1]. ∎

To provide the convergence and error bound results, we start by introducing some notations. If

$$W=(\cdots,\vec{W}_{-1},\vec{W}_0,\vec{W}_1,\cdots)=(\vec{W}_j)_{-\infty}^{+\infty}, \quad (3.2)$$

where each $\vec{W}_j$ is a vector, we define

$$\|W\|_2^2=\sum_{j=-\infty}^{+\infty}\|\vec{W}_j\|_2^2\Delta x, \quad (3.3)$$

where $\|\vec{W}_j\|_2$ represents the standard L^2-norm for a vector. We define the local truncation error of (2.16) as

$$\epsilon^n==(\vec{\epsilon}(j,n))_{j=-\infty}^{j=+\infty}=\begin{pmatrix}\epsilon_1(j,n)\\ \epsilon_2(j,n)\end{pmatrix}_{j=-\infty}^{j=+\infty}, n\geq 0, \quad (3.4)$$

where

$$\epsilon_1(j,n)=u(x_j,t^n)-\left[Q_+^2\begin{pmatrix}u(x_{j-1},t^n)\\ \frac{\Delta x}{4}u_x(x_{j-1},t^n)\end{pmatrix}+Q_{-1}^2\begin{pmatrix}u(x_{j+1},t^n)\\ \frac{\Delta x}{4}u_x(x_{j+1},t^n)\end{pmatrix}\right.$$
$$\left.+(Q_+Q_-+Q_-Q_+)\begin{pmatrix}u(x_j,t^n)\\ \frac{\Delta x}{4}u_x(x_j,t^n)\end{pmatrix}\right]_1, \quad (3.5)$$

$$\epsilon_2(j,n)=\frac{\Delta x}{4}u_x(x_j,t^n)-\left[Q_+^2\begin{pmatrix}u(x_{j-1},t^n)\\ \frac{\Delta x}{4}u_x(x_{j-1},t^n)\end{pmatrix}+Q_-^2\begin{pmatrix}u(x_{j+1},t^n)\\ \frac{\Delta x}{4}u_x(x_{j+1},t^n)\end{pmatrix}\right.$$

$$+ (Q_+Q_- + Q_-Q_+) \begin{pmatrix} u(x_j, t^n) \\ \frac{\Delta x}{4} u_x(x_j, t^n) \end{pmatrix} \Bigg]_2, \quad (3.6)$$

$$\begin{bmatrix} \xi \\ \zeta \end{bmatrix}_1 = \xi, \begin{bmatrix} \xi \\ \zeta \end{bmatrix}_2 = \zeta, \quad (3.7)$$

and $u(x,t)$ is the exact solution of (2.1). We now have the following results.

Lemma 3.2. *Let $u(x,t)$ be the exact solution of* (2.1)*, and we assume that $u(x,t)$ is sufficiently regular. Then for any n and j, we have*

$$\begin{aligned} \epsilon_1(j,n) \;=\; & \Delta t \left\{ \frac{1}{2} \left(u_{xx}(x_j,t^n) - a^2 u_{tt}(x_j,t^n)\right)\Delta t \right. \\ & + \frac{a}{6}\left[u_{xxx}(x_j,t^n)\Delta x^2 - \frac{3}{4}u_{xxxx}(x_j,t^n)\frac{(1-\tau^2-\delta)(\Delta x^2 - a^2\Delta t^2)}{1-\tau^2+\delta}\Delta t\right] \\ & \left. +\; C_1(\Delta t^3 + \Delta x^4)\right\}, \end{aligned} \quad (3.8)$$

$$\begin{aligned} \epsilon_2(j,n) \;=\; & \frac{4\delta(1-\tau^2)}{(1-\tau^2+\delta)^2}\Delta x \left\{ \frac{(1-\tau^2+\delta)^2}{16\mu(1-\tau^2)}\Delta x^2 u_{xt}(x_j,t^n) \right. \\ & - \frac{a(1-\tau^2-\delta)^2}{16\mu(1-\tau)^2}\Delta x^2 u_{xxx}(x_j,t^n) \\ & + \frac{a(1-\tau^2)}{8\mu}\Delta x^2 u_{xx}(x_j,t^n) + \frac{(1-\tau^2+\delta)^2}{4\delta(1-\tau^2)}\Delta t^2 \\ & + C_1\left(1+\frac{\tau}{\delta}(1-\tau^2)\right)\left(1+\frac{1-\tau^2-\delta}{1+\tau}\right)\Delta x^2 \\ & \left. + C_2\left(1-\frac{\tau}{\delta}(1-\tau^2)\right)\left(1+\frac{1-\tau^2-\delta}{1-\tau}\right)\Delta x^2\right\}, \end{aligned} \quad (3.9)$$

where C_1, C_2 are constants involving higher-order derivatives of $u(x,t)$ evaluated at some point near (x_j, t^n), but independent of the grid size and coefficients.

Proof. (3.8) and (3.9) can be obtained by the standard Taylor expansion under the assumption that $u(x,t)$ is sufficiently smooth. The proof is quite tedious and technical, and thus is omitted here. ∎

Next, we derive an error bound. Define the error vector between the exact solutions and approximate solutions at time level t^n as

$$E^n = (\cdots, \vec{E}(-1,n), \vec{E}(0,n), \vec{E}(1,n), \cdots) = (\vec{E}(j,n))_{j=-\infty}^{j=+\infty}, \quad (3.10)$$

where

$$\vec{E}(j,n) = \begin{pmatrix} u(x_j,t^n) - U_j^n \\ \frac{\Delta x}{4}\left[u_x(x_j,t^n) - (U_x)_j^n\right] \end{pmatrix}. \quad (3.11)$$

By combining (2.16), (3.5), and (3.6), we get

$$\vec{E}(j,n) = Q_+^2\vec{E}(j-1,n-1) + Q_-^2\vec{E}(j+1,n-1) + (Q_+Q_- + Q_-Q_+)\vec{E}(j,n-1) + \vec{\epsilon}(j,n). \quad (3.12)$$

The following theorem gives the error bound result.

Theorem 3.1. *Let T be a fixed time, and $u(x,t)$ be the exact solution of* (2.1)*, which is assumed to be sufficiently regular. Then for any $t^n \le T$, the $a-\mu$ scheme* (2.16) *is convergent, if the stability condition* (3.1) *is satisfied, and*

$$\begin{aligned}\|E^n\|_2 &= \left(\sum_{j=-\infty}^{+\infty} \|\vec{E}(x_j,t^n)\|_2^2 \Delta x\right)^{1/2} \\ &= \left(\sum_{j=-\infty}^{+\infty} \left[(u(x_j,t^n) - U_j^n)^2 + \left(\frac{\Delta x}{4}\left(u_x(x_j,t^n) - (U_x)_j^n\right)\right)^2\right]\Delta x\right)^{1/2} \\ &\le C^* T \max(\tau, a\tau,)\Delta x, \end{aligned} \quad (3.13)$$

where

$$C^{*2} = \|g(x,0)\|_{L^1(R^1)} + \Delta x\|g_x(x,0)\|_{L^1(R^1)} + \Delta x\|g_{xt}(x,t)\|_{L^1(R^1\times(0,T))} + \|g_t(x,t)\|_{L^1(R^1\times(0,T))}, \quad (3.14)$$

and

$$g(x,t) = \sum_{k=1}^{K}\sum_{0\le\alpha_k\le K} C_{\alpha_k}\left(\frac{\partial^k u(x,t)}{\partial x^{\alpha_k}\partial t^{k-\alpha_k}}\right)^2, \quad (3.15)$$

where C_{α_k} represents bounded positive constant independent of τ, δ, and K is a fixed positive integer. Since $u(x,t)$ is assumed to be sufficiently regular, C^* is a bounded, positive constant.

Proof. We first define a Fourier transform $\hat{E}^n(\theta)$ of E^n. For $\theta \in (-\pi, \pi]$, we define

$$\begin{aligned}\hat{E}^n(\theta) &= \frac{1}{\sqrt{2\pi}}\sum_{j=-\infty}^{+\infty} e^{-\mathbf{i}j\theta}\vec{E}(j,n) \\ &= \begin{pmatrix}\hat{E}_1^n(\theta)\\ \hat{E}_2^n(\theta)\end{pmatrix} \\ &= \begin{pmatrix}\frac{1}{\sqrt{2\pi}}\sum_{j=-\infty}^{+\infty} e^{-\mathbf{i}j\theta}(u(x_j,t^n) - U_j^n) \\ \frac{1}{\sqrt{2\pi}}\sum_{j=-\infty}^{+\infty} e^{-\mathbf{i}j\theta}\frac{\Delta x}{4}\left(u_x(x_j,t^n) - (U_x)_j^n\right)\end{pmatrix}, \end{aligned} \quad (3.16)$$

where $\mathbf{i} = \sqrt{-1}$. Then

$$\begin{aligned}\hat{E}^n(\theta) &= \frac{1}{\sqrt{2\pi}}\sum_{j=-\infty}^{+\infty} e^{-\mathbf{i}j\theta}(Q_+^2\vec{E}(j-1,n-1) \\ &\quad + Q_-^2\vec{E}(j+1,n-1) + (Q_+Q_- + Q_-Q_+)\vec{E}(j,n-1) + \vec{\epsilon}(j,n))\end{aligned}$$

$$
\begin{aligned}
&= Q(\theta)^2 \hat{E}^{n-1}(\theta) + \frac{1}{\sqrt{2\pi}} \sum_{j=-\infty}^{+\infty} e^{-\mathbf{i}j\theta} \vec{\epsilon}(j,n) \\
&= Q(\theta)^2 \hat{E}^{n-1}(\theta) + \hat{\epsilon}^n(\theta),
\end{aligned} \tag{3.17}
$$

where

$$
\begin{aligned}
Q(\theta) &= e^{-\mathbf{i}(\theta/2)} Q_+ + e^{\mathbf{i}(\theta/2)} Q_- \\
&= \begin{pmatrix} \cos\frac{\theta}{2} - \mathbf{i}\tau \sin\frac{\theta}{2} & -\mathbf{i}(1-\tau^2-\delta)\sin\frac{\theta}{2} \\ \mathbf{i}\frac{(1-\tau^2)\sin\frac{\theta}{2}}{1-\tau^2+\theta} & -\frac{1-\tau^2+\delta}{1-\tau^2+\delta}\left(\cos\frac{\theta}{2} + \mathbf{i}\tau\sin\frac{\theta}{2}\right) \end{pmatrix}
\end{aligned} \tag{3.18}
$$

and

$$
\begin{aligned}
\hat{\epsilon}^n(\theta) &= \frac{1}{\sqrt{2\pi}} \sum_{j=-\infty}^{+\infty} e^{-\mathbf{i}j\theta} \vec{\epsilon}(j,n) \\
&= \begin{pmatrix} \hat{\epsilon}_1^n(\theta) \\ \hat{\epsilon}_2^n(\theta) \end{pmatrix} = \begin{pmatrix} \frac{1}{\sqrt{2\pi}} \sum_{j=-\infty}^{+\infty} e^{-\mathbf{i}j\theta} \epsilon_1(j,n) \\ \frac{1}{\sqrt{2\pi}} \sum_{j=-\infty}^{+\infty} e^{-\mathbf{i}j\theta} \epsilon_2(j,n) \end{pmatrix}.
\end{aligned} \tag{3.19}
$$

From (3.17), we have that

$$
\begin{aligned}
\hat{E}^n(\theta) &= Q(\theta)^2 \hat{E}^{n-1}(\theta) + \hat{\epsilon}^n(\theta) \\
&= Q(\theta)^4 \hat{E}^{n-2}(\theta) + Q(\theta)^2 \hat{\epsilon}^{n-1}(\theta) + \hat{\epsilon}^n(\theta) \\
&= \cdots \\
&= (Q(\theta))^{2n} \hat{E}^0(\theta) + \sum_{l=1}^{n} (Q(\theta))^{n-l} \hat{\epsilon}^l(\theta).
\end{aligned} \tag{3.20}
$$

Clearly,

$$
\hat{E}^0(\theta) = \vec{0}. \tag{3.21}
$$

Thus, we have that

$$
\hat{E}^n(\theta) = \sum_{l=1}^{n} (Q(\theta)^2)^{n-l} \hat{\epsilon}^l(\theta). \tag{3.22}
$$

It is proved in [1] that, as long as the stability condition (3.1) is satisfied, then

$$
\|Q(\theta)\|_2 \leq 1.
$$

$\|Q(\theta)\|_2$ represents the matrix-2 norm of $Q(\theta)$. By using the fact that $\|E^n\|_2 = \|\hat{E}^n(\theta)\|_{L^2(-\pi,+\pi)}$ (see [3]), we have that

$$
\begin{aligned}
\|E^n\|_2 &= \|\hat{E}^n(\theta)\|_{L^2(-\pi,\pi)} = \left\| \sum_{l=1}^{n} (Q(\theta)^2)^{n-l} \hat{\epsilon}^l(\theta) \right\|_{L^2(-\pi,\pi)} \\
&\leq \sum_{l=1}^{n} \|Q(\theta)^{2(n-l)}\|_2 \|\hat{\epsilon}^l(\theta)\|_{L^2(-\pi,\pi)} = \sum_{l=1}^{n} \|Q(\theta)\|_2^{2(n-l)} \|\hat{\epsilon}^l(\theta)\|_{L^2(-\pi,\pi)} \\
&= \sum_{l=1}^{n} \|\epsilon^l\|_2 \Delta x^{1/2}
\end{aligned}
$$

$$= \sum_{l=1}^{n} \left(\sum_{j=-\infty}^{+\infty} |\epsilon_1(j,l)|^2 + |\epsilon_2(j,l)|^2 \Delta x \right)^{1/2}.$$

[by using the results of (3.8) and (3.9)]

$$\leq \left(a\Delta t^2 + a\Delta x^2 \Delta t + a^2 \Delta t^2 + \frac{\delta}{\mu}\Delta x^3 + \frac{a\delta}{\mu}\Delta x^3 + \frac{\delta}{\mu}\Delta x^3 + \Delta x \Delta t \right) \times \sum_{l=1}^{n} \left(\sum_{j=-\infty}^{+\infty} \sum_{k=1}^{K} \sum_{0 \leq \alpha_k \leq k} C_{\alpha_k} \left(\frac{\partial u^k}{\partial x^{\alpha_k} \partial t^{k-\alpha_k}} (x'_j, t^{n'}) \right)^2 \Delta x \right)^{1/2}, \quad (3.23)$$

where

$$\sum_{j=-\infty}^{+\infty} \sum_{k=1}^{K} \sum_{0 \leq \alpha_k \leq k} C_{\alpha_k} \left(\frac{\partial u^k}{\partial x^{\alpha_k} \partial t^{k-\alpha_k}} (x'_j, t^{n'}) \right)^2 \Delta x = \sum_{j=-\infty}^{+\infty} g(x'_j, t^{n'}) \Delta x. \quad (3.24)$$

In Appendix A, we prove that

$$\sum_{j=-\infty}^{+\infty} g(x'_j, t^{n'}) \Delta x \leq C^{*2}. \quad (3.25)$$

So, we get from (3.23) that

$$\begin{aligned} \|E^n\|_2 &\leq C^* n \left(a\Delta t^2 + a\Delta x^2 \Delta t + a^2 \Delta t^2 + \frac{\delta}{\mu}\Delta x^3 + \Delta x \Delta t \right) \\ &\leq C^* T \frac{1}{\Delta t} \left(a\Delta t^2 + a\Delta x^2 \Delta t + a^2 \Delta t^2 + \frac{\delta}{\mu}\Delta x^3 + \Delta x \Delta t \right). \end{aligned} \quad (3.26)$$

If we use the definition

$$\tau = \frac{a\Delta t}{\Delta x}, \delta = \frac{4\mu \Delta t}{\Delta x^2},$$

and plug them into (3.26), then (3.13) follows. ∎

Remark 3.1. *As described in Lemma* 3.1, *the* $a - \mu$ *scheme is not sensitive to* μ. *Our numerical results confirm this*.

Remark 3.2. *Theorem* 3.2 *shows several unusual features regarding the convergent behavior of* $a - \mu$ *scheme*:

I) *Other than the stability condition for* $\Delta x, \Delta t$, *there are no further requirements for* Δx *or* Δt *regarding the convergence of* $a - \mu$ *scheme*.
II) *The error bound or convergence rate does not depend on* μ. *This is confirmed by our numerical experiments*.
III) *The error bound depends on* T. *But unlike standard schemes for time-dependent cases, which involve a factor of* e^T, *the dependence is linear*.
IV) *As required by the stability result,* τ *satisfies* $0 < \tau < 1$, *so the factor* $\max(\tau, a\tau)$ *in* (3.13) *is really bounded by* $\max(a, 1)$, *which is a fixed constant*.

Remark 3.3. *Theorem* 3.2 *indicates that the global convergence rate for the solution in the* L^2 *space norm is of order* Δx, *but we cannot conclude any global convergence rate for its derivative*.

TABLE I. Relative errors between exact solution and numerical solution for Example 4.1 with different diffusion coefficients. The temporal grid size $\Delta t = 0.9\Delta x$. Simulation ends at $T = 1.5$.

	$\mu = 1$		$\mu = 10^{-2}$		$\mu = 10^{-4}$	
Δx	Solution	Derivative	Solution	Derivative	Solution	Derivative
0.04	4.92e-05	3.37e-05	4.15e-05	2.62e-04	4.33e-05	2.58e-04
0.02	1.21e-05	8.17e-06	1.03e-05	5.64e-05	1.07e-05	6.06e-05
0.01	3.02e-06	2.03e-06	2.57e-06	1.40e-05	2.68e-06	1.51e-05
0.005	7.51e-07	5.05e-07	6.41e-07	3.39e-06	6.68e-07	3.65e-06

IV. NUMERICAL EXPERIMENTS

In this section, numerical experiments are conducted to support our results in previous sections. In particular, we want to show numerically that the method performs well for small and large Peclet numbers and for short and long simulation time as mentioned in Remark 3.2.

In the following experiments, we show relative errors between the exact solution and numerical solution in the $L^\infty(0,T;L^2[b,d])$ norm:

$$\text{solution error } = \frac{\max_{0\le t_n\le T}\left(\int_b^d |u(t_n,x)-U^n(x)|^2dx\right)^{1/2}}{\max_{0\le t_n\le T}\left(\int_b^d |u(t_n,x)|^2dx\right)^{1/2}}, \tag{4.1}$$

$$\text{derivative error } = \frac{\max_{0\le t_n\le T}\left(\int_b^d \left|\frac{\partial u(t_n,x)}{\partial x}-U_x^n(x)\right|^2dx\right)^{1/2}}{\max_{0\le t_n\le T}\left(\int_b^d \left|\frac{\partial u(t_n,x)}{\partial x}\right|^2dx\right)^{1/2}}, \tag{4.2}$$

where the integration in space is evaluated by the composite trapezoidal rule, and U^n, U_x^n are, respectively, the approximate solution and its derivative at t^n.

Example 4.1. *Find u satisfying*

$$\frac{\partial u}{\partial t} + a\frac{\partial u}{\partial x} - \mu\frac{\partial u^2}{\partial x^2} = f(x,t), (x,t) \in (b,d)\times(0,T], \tag{4.3}$$

$$u(b,t) = g_0, \frac{\partial u}{\partial x}(d,t) = g_1, t \in [0,T], \tag{4.4}$$

TABLE II. Relative errors between exact solution and numerical solution for Example 4.1 with different diffusion coefficients. The temporal grid size $\Delta t = 0.9\Delta x$. Simulation ends at $T = 1.5$.

	$\mu = 10^{-6}$		$\mu = 10^{-10}$		$\mu = 10^{-15}$	
Δx	Solution	Derivative	Solution	Derivative	Solution	Derivative
0.04	4.34e-05	1.25e-04	4.34e-05	1.25e-04	4.34e-05	1.25e-04
0.02	1.07e-05	3.08e-05	1.07e-05	3.05e-05	1.07e-05	3.05e-05
0.01	2.68e-06	8.85e-06	2.68e-06	7.60e-06	2.68e-06	7.60e-06
0.005	6.68e-07	3.11e-06	6.68e-07	1.89e-06	6.68e-07	1.89e-06

TABLE III. Relative errors between exact solution and numerical solution for Example 4.1 with different diffusion coefficients. The temporal grid size $\Delta t = 0.9\Delta x$. Simulation ends at $T = 1.5$.

	$\mu = 10^{-20}$		$\mu = 10^{-50}$		$\mu = 10^{-100}$	
Δx	Solution	Derivative	Solution	Derivative	Solution	Derivative
0.04	4.34e-05	1.25e-04	4.34e-05	1.25e-04	4.34e-05	1.25e-04
0.02	1.07e-05	3.05e-05	1.07e-05	3.05e-05	1.07e-05	3.05e-05
0.01	2.68e-06	7.60e-06	2.68e-06	7.60e-06	2.68e-06	7.60e-06
0.005	6.68e-07	1.89e-06	6.68e-07	1.89e-06	6.68e-07	1.89e-06

TABLE IV. Relative errors between exact solution and numerical solution for Example 4.1 with different diffusion coefficients. The temporal grid size $\Delta t = 0.9\Delta x$. Simulation ends at $T = 6.0$.

	$\mu = 1$		$\mu = 10^{-6}$		$\mu = 10^{-100}$	
Δx	Solution	Derivative	Solution	Derivative	Solution	Derivative
0.04	4.83e-05	4.02e-05	6.59e-05	1.08e-04	6.59e-05	1.08e-04
0.02	1.20e-05	1.00e-05	1.64e-05	2.70e-05	1.64e-05	2.68e-05
0.01	3.00e-06	2.50e-06	4.11e-06	1.00e-05	4.11e-06	6.70e-06
0.005	7.50e-07	6.26e-07	1.03e-06	4.14e-06	1.03e-06	1.67e-06

$$u(x, 0) = u_0(x), x \in [b, d], \tag{4.5}$$

where $[b, d] = [0, 1], a = 1$, *and the source function* $f(x, t)$ *and boundary values* g_0 *and* g_1 *are chosen such that the exact solution is* $u(x, t) = \sin(x+t)$. *Many values for the ending simulation time* T *and for the diffusion coefficient* μ *are given in the numerical results*.

Tables I–III and IV–VI show the errors in the solution and its derivative for various simulation ending times, $T = 1.5, T = 6.0, T = 12.0$, and $T = 24.0$ for Example 4.1. Note that the orders of convergence are consistent with our theorem. We do not observe any indication from the results that the accuracy deteriorates with the Peclet number and time; this is also consistent with our results.

When the convergence condition is violated, for example, when $a\Delta t/\Delta x = 1$, the convergence can be unpredictable, see Tables VII and VIII. The conclusion is, when the convergence condition is violated, the accuracy can still be good for convection-equal-to-diffusion problems, but can be arbitrarily bad for convection-dominated-diffusion problems.

TABLE V. Relative errors between exact solution and numerical solution for Example 4.1 with different diffusion coefficients. The temporal grid size $\Delta t = 0.9\Delta x$. Simulation ends at $T = 12.0$.

	$\mu = 1$		$\mu = 10^{-6}$		$\mu = 10^{-100}$	
Δx	Solution	Derivative	Solution	Derivative	Solution	Derivative
0.04	4.80e-05	4.01e-05	6.58e-05	1.08e-04	6.58e-05	1.08e-04
0.02	1.20e-05	1.00e-05	1.64e-05	2.70e-05	1.64e-05	2.68e-05
0.01	3.00e-06	2.50e-06	4.11e-06	9.96e-06	4.11e-06	6.69e-06
0.005	7.50e-07	6.26e-07	1.03e-06	4.14e-06	1.03e-06	1.67e-06

TABLE VI. Relative errors between exact solution and numerical solution for Example 4.1 with different diffusion coefficients. The temporal grid size $\Delta t = 0.9\Delta x$. Simulation ends at $T = 24.0$.

	$\mu = 1$		$\mu = 10^{-6}$		$\mu = 10^{-100}$	
Δx	Solution	Derivative	Solution	Derivative	Solution	Derivative
0.04	4.80e-05	4.01e-05	6.58e-05	1.08e-04	6.58e-05	1.08e-04
0.02	1.20e-05	1.00e-05	1.64e-05	2.70e-05	1.64e-05	2.68e-05
0.01	3.00e-06	2.50e-06	4.11e-06	9.96e-06	4.11e-06	6.69e-06
0.005	7.50e-07	6.26e-07	1.03e-06	4.13e-06	1.03e-06	1.67e-06

TABLE VII. Relative errors between exact solution and numerical solution for Example 4.1 with different diffusion coefficients. The temporal grid size $\Delta t = \Delta x$, which violates the convergence condition and leads to unpredictable results for the derivative. Simulation ends at $T = 1.5$.

	$\mu = 1$		$\mu = 10^{-4}$		$\mu = 10^{-100}$	
Δx	Solution	Derivative	Solution	Derivative	Solution	Derivative
0.04	5.86e-05	4.07e-05	1.72e+16	5.64e+19	1.35e-05	7.60e+12
0.02	1.43e-05	9.83e-06	9.18e-06	5.71e-02	1.60e-05	3.46e+12
0.01	3.58e-06	2.44e-06	2.29e-06	1.42e-02	7.78e-07	7.09e+11
0.005	8.95e-07	6.10e-07	5.74e-07	3.54e-03	3.73e-06	7.32e+12

Example 4.2. *Find u satisfying*

$$\frac{\partial u}{\partial t} + a\frac{\partial u}{\partial x} - \mu\frac{\partial u^2}{\partial x^2} = f(x,t), (x,t) \in (b,d) \times (0,T], \tag{4.6}$$

$$u(b,t) = g_0, \frac{\partial u}{\partial x}(d,t) = g_1, t \in [0,T], \tag{4.7}$$

$$u(x,0) = u_0(x), x \in [b,d], \tag{4.8}$$

where $[b,d] = [0,1], a = 1$, and the source function $f(x,t)$ and boundary values g_0 and g_1 are chosen such that the exact solution is $u(x,t) = e^{x+t}$. Many values for the ending simulation time T and for the diffusion coefficient μ are given in the numerical results.

Numerical results for Example 4.2 are shown in Tables IX–XII for simulation ending times at $T = 1, T = 10, T = 100$, and $T = 300$, and Peclet numbers $1, 10^6$, and 10^{100}, respectively. Clearly the accuracy does not show any deterioration with respect to time. It seems that there

TABLE VIII. Relative errors between exact solution and numerical solution for Example 4.1 with different diffusion coefficients. The temporal grid size $\Delta t = 1.5\Delta x$, which violates the convergence condition and leads to unpredictable results. Simulation ends at $T = 5.0$.

	$\mu = 1$		$\mu = 10^{-4}$		$\mu = 10^{-100}$	
Δx	Solution	Derivative	Solution	Derivative	Solution	Derivative
0.04	1.32e-04	1.36e-04	9.77e+61	8.82e+63	1.56e+61	1.38e+63
0.02	3.31e-05	3.41e-05	9.39e+132	1.72e+135	4.84e+129	8.60e+131
0.01	3.02e-05	3.57e-05	Infinity	Infinity	Infinity	Infinity
0.005	7.55e-06	8.92e-06	Infinity	Infinity	Infinity	Infinity

TABLE IX. Relative errors between exact solution and numerical solution for Example 4.2 with different diffusion coefficients. The temporal grid size $\Delta t = 0.9\Delta x$. Simulation ends at $T = 1.0$.

	$\mu = 1$		$\mu = 10^{-6}$		$\mu = 10^{-100}$	
Δx	Solution	Derivative	Solution	Derivative	Solution	Derivative
0.04	2.04e-05	1.29e-05	4.42e-05	5.63e-05	4.42e-05	4.56e-05
0.02	5.10e-06	3.14e-06	1.09e-05	1.77e-05	1.09e-05	1.12e-05
0.01	1.27e-06	7.77e-07	2.69e-06	7.27e-06	2.69e-06	2.78e-06
0.005	3.18e-07	1.94e-07	6.73e-07	3.27e-06	6.73e-07	6.94e-07

TABLE X. Relative errors between exact solution and numerical solution for Example 4.2 with different diffusion coefficients. The temporal grid size $\Delta t = 0.9\Delta x$. Simulation ends at $T = 10.0$.

	$\mu = 1$		$\mu = 10^{-6}$		$\mu = 10^{-100}$	
Δx	Solution	Derivative	Solution	Derivative	Solution	Derivative
0.04	1.85e-05	1.29e-05	4.32e-05	2.26e-05	4.32e-05	1.59e-05
0.02	4.63e-06	3.22e-06	1.08e-05	1.02e-05	1.08e-05	3.96e-06
0.01	1.16e-06	8.06e-07	2.69e-06	6.10e-06	2.69e-06	9.90e-07
0.005	2.89e-07	2.01e-07	6.73e-07	3.14e-06	6.73e-07	2.48e-07

is a slight deterioration in accuracy when the diffusion coefficient is decreased from 1 to 10^{-6}. However, when the diffusion coefficient is further decreased from 10^{-6} to 10^{-100}, the accuracy remains the same. Besides, the solution and its derivative are approximated at the same time with about the same accuracy. As for Example 4.1, the accuracy remains the same when the simulation ending time T is increased. This implies good long-time behavior of the numerical solution obtained by the space-time CESE scheme.

TABLE XI. Relative errors between exact solution and numerical solution for Example 4.2 with different diffusion coefficients. The temporal grid size $\Delta t = 0.9\Delta x$. Simulation ends at $T = 100.0$.

	$\mu = 1$		$\mu = 10^{-6}$		$\mu = 10^{-100}$	
Δx	Solution	Derivative	Solution	Derivative	Solution	Derivative
0.04	1.85e-05	1.29e-05	4.31e-05	2.23e-05	4.31e-05	1.58e-05
0.02	4.63e-06	3.22e-06	1.08e-05	1.01e-05	1.08e-05	3.96e-06
0.01	1.16e-06	8.05e-07	2.69e-06	6.09e-06	2.69e-06	9.90e-07
0.005	2.89e-07	2.01e-07	6.73e-07	3.13e-06	6.73e-07	2.47e-07

TABLE XII. Relative errors between exact solution and numerical solution for Example 4.2 with different diffusion coefficients. The temporal grid size $\Delta t = 0.9\Delta x$. Simulation ends at $T = 300.0$.

	$\mu = 1$		$\mu = 10^{-6}$		$\mu = 10^{-100}$	
Δx	Solution	Derivative	Solution	Derivative	Solution	Derivative
0.04	1.85e-05	1.29e-05	4.31e-05	2.22e-05	4.31e-05	1.58e-05
0.02	4.63e-06	3.22e-06	1.08e-05	1.01e-05	1.08e-05	3.96e-06
0.01	1.16e-06	8.05e-07	2.69e-06	6.09e-06	2.69e-06	9.90e-07
0.005	2.89e-07	2.01e-07	6.73e-07	3.13e-06	6.73e-07	2.47e-07

APPENDIX A

In this appendix, we prove Eq. (3.25), which is

$$\sum_{j=-\infty}^{+\infty} g(x'_j, t^{n'})\Delta x \le C^*, \tag{A1}$$

where x'_j is some point in $(x_{j-1}, x_j]$, $t^{n'}$ is some point in $(t^{n-1}, t^n]$. C^* is a positive constant defined in (3.14). Notice that $g(x,t)$ is a sufficiently regular and positive function.

Proof. We start with

$$\sum_{j=-\infty}^{+\infty} g(x'_j, t^{n'})\Delta x - \int_{-\infty}^{+\infty} g(x,0)\,dx = I + II, \tag{A2}$$

where

$$I = \sum_{j=-\infty}^{+\infty} g(x'_j, t^{n'})\,\Delta x - \sum_{j=-\infty}^{+\infty} g(x'_j, 0)\Delta x; \tag{A3}$$

$$\begin{aligned} II &= \sum_{j=-\infty}^{+\infty} g(x'_j, 0)\Delta x - \int_{-\infty}^{+\infty} g(x,0)\,dx \\ &= \sum_{j=-\infty}^{+\infty} \int_{x_j}^{x_{j+1}} (g(x'_j, 0) - g(x,0))\,dx. \end{aligned} \tag{A4}$$

Then

$$\begin{aligned} I &= \sum_{j=-\infty}^{+\infty} \int_0^{t^{n'}} g_t(x'_j, t)\,dt\,\Delta x \\ &= \sum_{j=-\infty}^{+\infty} \int_{x_j}^{x_{j+1}} \int_0^{t^{n'}} (g_t(x'_j, t) - g_t(x,t))\,dt\,dx + \sum_{j=-\infty}^{+\infty} \int_{x_j}^{x_{j+1}} \int_0^{t^{n'}} g_t(x,t)\,dxdt \\ &= \sum_{j=-\infty}^{+\infty} \int_{x_j}^{x_{j+1}} \int_0^{t^{n'}} \int_x^{x'_j} g_{xt}(w,t)\,dw\,dx\,dt + \sum_{j=-\infty}^{+\infty} \int_{x_j}^{x_{j+1}} \int_0^{t^{n'}} g_t(x,t)\,dx\,dt. \end{aligned} \tag{A5}$$

So

$$\begin{aligned} |I| &\le \Delta x \sum_{j=-\infty}^{+\infty} \int_{x_j}^{x_{j+1}} \int_0^T |g_{xt}(x,t)|\,dx\,dt + \sum_{j=-\infty}^{+\infty} \int_{x_j}^{x_{j+1}} \int_0^T |g_t(x,t)|\,dx\,dt \\ &= \Delta x \|g_{xt}\|_{L^1(R^1\times[0,T])} + \|g_t\|_{L^1(R^1\times[0,T])}. \end{aligned} \tag{A6}$$

We now estimate II:

$$\begin{aligned} |II| &= \left| \sum_{j=-\infty}^{+\infty} \int_{x_j}^{x_{j+1}} \int_x^{x'_j} g_x(w,0)\,dw\,dx \right| \\ &\le \Delta x \sum_{j=-\infty}^{+\infty} \int_{x_j}^{x_{j+1}} |g_x(w,0)|\,dw = \Delta x \|g_x(x,0)\|_{L^1(R)}. \end{aligned} \tag{A7}$$

Equation (3.25) follows from (A.6) and (A.7). ■

References

1. Sin-Chung Chang, The method of space-time conservation element and solution element—A new approach for solving the Navier–Stokes and Euler equations, J Comp Ph 119 (1995), 295–324.
2. S. C. Chang and W. M. To, NASA TM 104495, August 1991 (unpublished).
3. B. Noble and J. W. Daniel, Applied linear algebra, 2nd Ed., Prentice–Hall, Englewood Cliffs, NJ, 1977.
4. J. W. Thomas, Numerical partial differential equations, Springer–Verlag, New York, 1995.